

Strain engineering enhancement of surface plasmon polariton propagation lengths for gold nanowires

Xue Ben and Harold S. Park

Citation: *Appl. Phys. Lett.* **102**, 041909 (2013); doi: 10.1063/1.4790293

View online: <http://dx.doi.org/10.1063/1.4790293>

View Table of Contents: <http://apl.aip.org/resource/1/APPLAB/v102/i4>

Published by the [American Institute of Physics](http://www.aip.org).

Related Articles

Electroluminescence from spatially confined exciton polaritons in a textured microcavity

Appl. Phys. Lett. **102**, 041101 (2013)

Large area sub-wavelength azo-polymer gratings by waveguide modes interference lithography

Appl. Phys. Lett. **102**, 031103 (2013)

Attenuated total reflection study of bulk and surface polaritons in antiferromagnets and hexagonal ferrites: Propagation at arbitrary angles

J. Appl. Phys. **113**, 013904 (2013)

Polariton multistability and fast linear-to-circular polarization conversion in planar microcavities with lowered symmetry

Appl. Phys. Lett. **102**, 011104 (2013)

Probing molecular interactions on carbon nanotube surfaces using surface plasmon resonance sensors

Appl. Phys. Lett. **101**, 223114 (2012)

Additional information on *Appl. Phys. Lett.*

Journal Homepage: <http://apl.aip.org/>

Journal Information: http://apl.aip.org/about/about_the_journal

Top downloads: http://apl.aip.org/features/most_downloaded

Information for Authors: <http://apl.aip.org/authors>

ADVERTISEMENT

AIP | Applied Physics
Letters

SURFACES AND INTERFACES
Focusing on physical, chemical, biological, structural, optical, magnetic and electrical properties of surfaces and interfaces, and more...

ENERGY CONVERSION AND STORAGE
Focusing on all aspects of static and dynamic energy conversion, energy storage, photovoltaics, solar fuels, batteries, capacitors, thermoelectrics, and more...

EXPLORE WHAT'S NEW IN APL

SUBMIT YOUR PAPER NOW!

The advertisement features a 3D schematic of a device structure on the left, showing a 1µm-thick LPCVD Silicon Dioxide layer, a Ground Ring, a Metal Vias, a Drain, a Source, and a QDs region. On the right, there is a diagram illustrating energy conversion and storage, showing a QDs region, a CIGS layer, and a NO₂ molecule.

Strain engineering enhancement of surface plasmon polariton propagation lengths for gold nanowires

Xue Ben and Harold S. Park^{a)}

Department of Mechanical Engineering, Boston University, Boston, Massachusetts 02215, USA

(Received 18 October 2012; accepted 21 January 2013; published online 30 January 2013)

We present in this work the notion of using elastic strain engineering to reduce the intrinsic losses in a metal for subwavelength optical signal processing. By using a simple, analytical waveguide model, we demonstrate that application of uniaxial tensile strains below the yield strain of gold nanowires results in substantial increases of more than 70% in the surface plasmon polariton propagation lengths at optical frequencies. The enhancement is primarily due to a reduction in the core electron density, and is found to be size-independent for a wide range of nanowire diameters, while exhibiting a linear dependence on the applied tensile strain. © 2013 American Institute of Physics. [<http://dx.doi.org/10.1063/1.4790293>]

Surface plasmons (SPs) are associated with the collective motion of electrons, and exist at a metal-dielectric interface for metals such as gold and silver.^{1–3} Surface plasmon polaritons (SPPs), which are the coupled excitations of photons and SPs at a metal surface, and thus concentrate electromagnetic energy at the nanometer scale, are one solution to overcoming the diffraction limit.^{4,5} Importantly, SPPs may allow the development of optical devices that can carry and control light signals to different parts of a nanophotonic circuit on a sub-wavelength scale.^{6–12}

However, the electromagnetic energy confined at the metal-dielectric interface exhibits an exponential decay in the direction of SPP propagation, which limits the maximum propagation length of light for subwavelength guiding. Therefore, one fundamental issue that must be overcome for SPP-based nanophotonic circuits is losses associated with this resistive heating in metals. In particular, the high propagation losses related to SPPs at optical frequencies pose a substantial hurdle for SPP-based devices for subwavelength optical signal processing.¹³

One approach to reducing the resistive heating losses that arise from the imaginary portion of the dielectric function, and thus increasing the propagation length, is to reduce the loss inside a metallic material. For example, a metal-air-substrate structure can be adopted because a large portion of energy is confined in the substrate, in which case no significant propagation loss will occur in the metal.¹⁴ Alternatively, waveguide structures have recently been developed with the underlying idea of achieving a longer SPP propagation length.^{15,16} However, these approaches to reducing losses typically come with a lower degree of energy confinement.

Therefore, intrinsic losses in the metal are the dominant factor causing SPP propagation losses in metal nanowires, with scattering or surface damping a minor contributor. If larger optical signal transfer lengths are desired without losing strong field localization, one must take a fundamental approach to reducing the loss of the metal while still keeping it metallic. For example, Khurgin and Sun¹⁷ recently proposed that metals could become lossless in the mid-IR or higher

wavelengths if the lattice spacing in the metal is doubled. However, it appears to be difficult at present to design metals with such requirements on their lattice spacing.

Because of this, we present here a different approach to reducing the losses in gold nanowires due to changing the lattice spacing—that of applied tensile mechanical strain. While gold is intrinsically more lossy than silver, particularly at optical frequencies,¹⁸ it is studied more widely because silver is chemically unstable at ambient conditions.¹⁹ We demonstrate that changes in the core electron density due to applied tensile strain enable substantial enhancements in the SPP propagation length at optical frequencies. The present work thus provides a different perspective in designing and fabricating gold nanoplasmonic devices to support efficient optical signal transfer.

The optical response of metal nanostructures is often modeled using the bulk Drude model for the free electrons in the conduction band²⁰ and a core term to account for the contribution of bound electrons. The resulting dielectric function $\epsilon(\omega)$ that emerges is

$$\epsilon(\omega) = \epsilon_{core}(\omega) + \epsilon_{free}(\omega) - 1, \quad (1)$$

where the free electron term is expressed as Drude model,

$$\epsilon_{free}(\omega) = 1 - \frac{\omega_p^2}{\omega(\omega + i\gamma)}, \quad (2)$$

and where $\omega_p = (ne^2/\epsilon_0 m_{eff})$ is the plasma frequency, n is the electron density, m_{eff} is the effective mass, and γ is the collision frequency, which is related to electron scattering processes. ϵ_{core} accounts for interband transitions, and is related to the core-electron polarizability, and thus the core electron density.

The phenomenon we are interested in capturing and modeling is the change in lattice spacing, and thus electron density that occurs for both the free and core electrons as a result of axial strain-induced stretching of the gold nanowires.^{21–23}

For the strain-induced modification of the core electron term, we assume following Sturm *et al.*²⁴ that the core polarizability $\alpha_{core}(\omega)$, which is dependent on the atomic localized orbitals, is assumed to be unchanged by mechanical strain.²⁵ Thus, an axial strain ζ only adds a perturbation to

^{a)}Electronic address: parkhs@bu.edu.

the core electron density n_c , which in turn changes ϵ_{core} . Because of this, we can write the core electron permittivity as a function of uniaxial tensile strain ζ as

$$\epsilon_{core}(\omega, \zeta) = \frac{(1 + \zeta)(\epsilon_{core}(\omega) + 2) + 2(\epsilon_{core}(\omega) - 1)}{(1 + \zeta)(\epsilon_{core}(\omega) + 2) - (\epsilon_{core}(\omega) - 1)}. \quad (3)$$

Because the deformation in the nanowires is predominately axial, we ignore dimensional changes of the nanowire in the transverse directions.

Treating strain effects on the free electron term is considerably simpler.²⁶ Specifically, an increase in the lattice constant decreases the free electron density n , and thus the plasmon frequency. For FCC metals under uniaxial tensile strain ζ , we have

$$\omega_p(\zeta) = \frac{4e^2}{\epsilon_0 m_{eff} a_0^3 (1 + \zeta)}, \quad (4)$$

where e is the electric charge and $a_0 = 4.08 \text{ \AA}$ is the bulk lattice constant for gold.

Before introducing the analytical waveguide model and the corresponding numerical results, we summarize the procedure used to calculate the strain-dependent dielectric functions in Eqs. (1)–(4). We first took the bulk dielectric constants obtained by Johnson and Christy,²⁷ and calculated the free electron contribution $\epsilon_{free}(\omega)$ using Eq. (2), with $\omega_p = \frac{4e^2}{\epsilon_0 m_{eff} a_0^3}$, $\gamma = \frac{1}{\tau}$. The parameters $\tau = 9.3 \times 10^{-15}$, the relaxation time for gold in seconds, and the effective electron mass $m_{eff} = 0.99m_0$, where m_0 is the mass of an electron, were again both obtained from the experimental work of Johnson and Christy.²⁷ The lattice constant for gold was taken to be $a_0 = 4.08 \text{ \AA}$. We then subtract the free electron contribution $\epsilon_{free}(\omega)$ from the experimental data $\epsilon(\omega)$ using Eq. (1) to obtain $\epsilon_{core}(\omega)$. The strain-modifications can then be performed using Eqs. (3) for $\epsilon_{core}(\omega)$, and putting Eq. (4) in Eq. (2) for $\epsilon_{free}(\omega)$.

We note that because we consider gold nanowires with radii ranging from 20 to 100 nm in this work, it is safe to apply the above modifications to the free and core electron densities based on classical theories. We also note that these nanowire sizes are also large enough such that surface damping effects²⁸ and quantum effects can safely be neglected. We also considered tensile elastic strains ranging from 1% to 5%. These values were considered as they have been achieved both experimentally,^{29–31} and also in classical molecular dynamics simulations of metal nanowires^{32–34} without the onset of yield, and thus the nucleation and propagation of planar defects such as dislocations or twins.

To calculate the SPP propagation lengths in gold nanowires, we use the recently developed analytical waveguide model.¹⁹ This model considers a circular nanowire with infinite length embedded in a homogeneous dielectric medium. It was also noted¹⁹ that although only the fundamental mode of the nanowire was obtained, quantitative agreement was obtained between the analytic theory, numerical finite difference time domain (FDTD) simulations, and experiments. Because only the lowest-order waveguide mode is considered, we can determine the propagation length by solving the following equations:^{19,35}

$$\begin{aligned} \frac{\epsilon(\omega, \zeta) J_1(KR)}{KR J_0(KR)} &= \frac{\epsilon_d H_1^{(1)}(K_d R)}{K_d R H_0^{(1)}(K_d R)}, \\ K^2 &= \frac{\epsilon(\omega, \zeta) \omega^2}{c^2} - h^2, \\ K_d^2 &= \frac{\epsilon_d \omega^2}{c^2} - h^2, \\ h &= k_{spp} + i\alpha, \\ L_{prop} &= \frac{1}{2\alpha}, \end{aligned} \quad (5)$$

where ϵ_d is the dielectric constant of the surrounding medium, R is the radius of the nanowire, c is the speed of light in vacuum, K and K_d are the wavevectors in gold and the dielectric medium, respectively, J_i are ordinary Bessel functions of order i , H_i are Hankel functions of order i , and h , the complex propagation constant, is the quantity we are interested in solving for in order to obtain L_{prop} . The real part k_{spp} of the propagation constant h represents the oscillating wave, while the imaginary part α describes the decay of the optical energy propagating along the nanowire. The above Eqs. (5) make clear the dependence of the complex propagation constant h on the strain ζ . We refer readers to Wild *et al.*¹⁹ for details in choosing the solutions of the above equations.

We now show results obtained using the analytical waveguide model in Eqs. (5) along with the strain-modified dielectric functions in Eqs. (3) and (4) to examine the enhancement in SPP propagation length in gold nanowires. For maximum generality, we consider nanowires with radii ranging from 20 to 100 nm subject to uniaxial tensile strains ranging from 1% to 5% for each diameter.

To quantify the effectiveness of the applied strain in changing the SPP propagation lengths, we define a quantity η , the propagation length enhancement factor

$$\eta = \frac{L_{prop}^{strain} - L_{prop}}{L_{prop}}, \quad (6)$$

where L_{prop}^{strain} is the SPP propagation length when tensile mechanical strain is applied, and L_{prop} is the propagation length without strain.

We show in Fig. 1 the strain-dependence of the SPP propagation length enhancement for a gold nanowire of

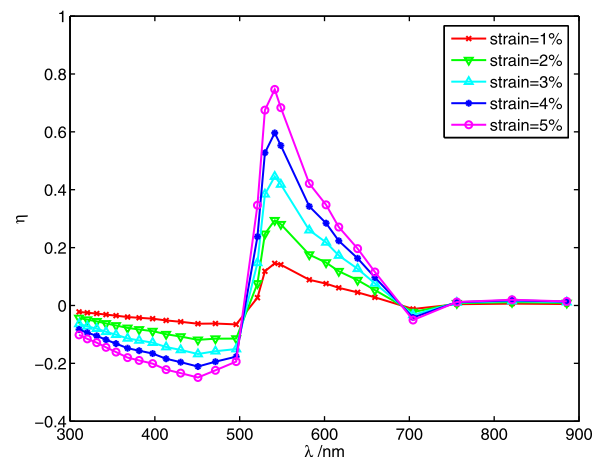


FIG. 1. SPP propagation length improvement factor η for circular gold nanowires of diameter 120 nm under axial tensile strains ranging from 1% to 5%.

diameter 120 nm for uniaxial tensile strains ranging from 1% to 5%. Fig. 1 shows that there is a consistent increase in η as the tensile strain increases, and that the SPP propagation length enhancement reaches a maximum for all strains around a wavelength of $\lambda = 540$ nm. Because the enhancement factor η was calculated from the experimental values of Johnson and Christy,²⁷ we performed an estimation of the error for η at each level of strain, and found that the maximum error in η at its maximum value (i.e., around 540 nm in Fig. 1) for any strain level is smaller than 2%. While the error is larger at other wavelengths due to the increase in experimental error away from the surface plasmon resonance wavelength,²⁷ the peak enhancement is our primary interest in this work, and, therefore, the trends reported in this work are unaffected.

We quantify the dependence of the maximum SPP propagation length enhancement η as a function of applied tensile strain ζ in Fig. 2. There, we show for a range of nanowire radii from 20 to 100 nm that the enhancement is linear as a function of strain, and that the difference in maximum enhancement shows only a small reduction as the nanowire diameter decreases, i.e., that the strain-induced enhancement in SPP propagation length is essentially size-independent.

To gain further insights as to whether the core or free electron density reduction is responsible for the observed SPP propagation length enhancement, we performed a systematic study to separate the two effects, for which the results are shown in Fig. 3. As shown in Fig. 3, the reduction in the core and free electron densities does not mean both contribute in a positive fashion in reducing the SPP propagation loss. For the optical frequency range shown in Fig. 3, the reduction in core electron density can be seen to strongly reduce the intrinsic metallic losses, thus increasing the SPP propagation length, with an increase in enhancement with strain. In contrast, a reduction in the free electron density, as described by the classical Drude model, works in the opposite fashion, where the SPP propagation length is decreased with increasing strain. While the free electron density reduction results in a decrease in propagation length, the magnitude of the decrease is small compared to the increase resulting from the decrease in the core electron density, and

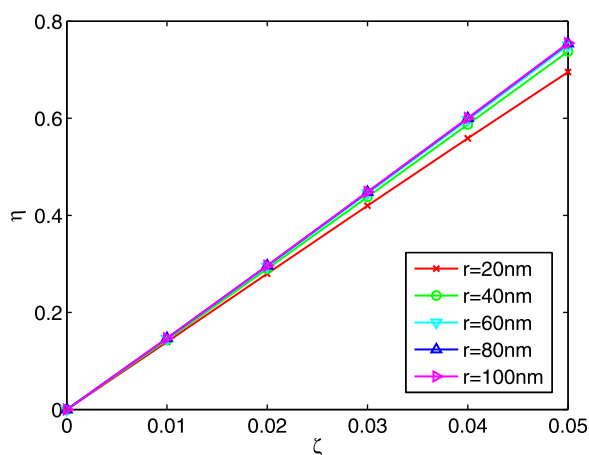


FIG. 2. Maximum SPP propagation length improvement factors η for circular gold nanowires with radii from 20 to 100 nm under axial tensile strains from 1% to 5%.

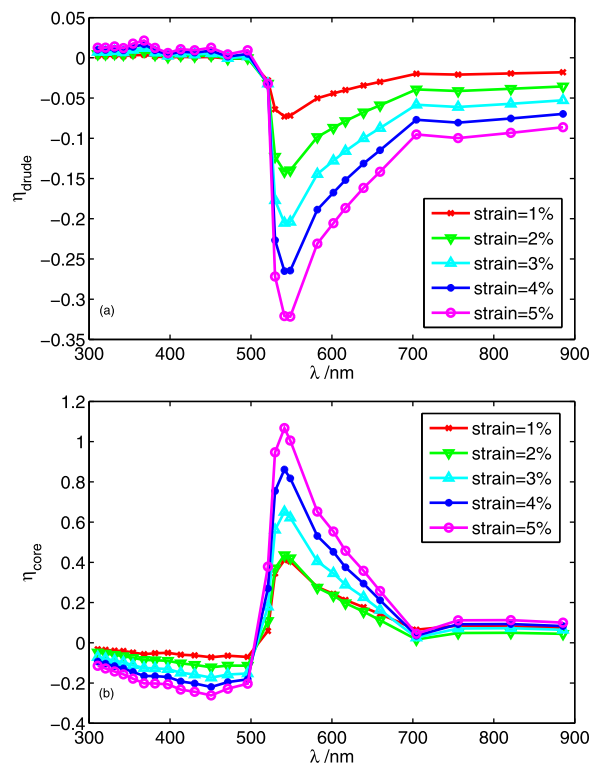


FIG. 3. SPP propagation length enhancement factors for circular gold nanowires with radius 60 nm under tensile strains ranging from 1% to 5%. (a) Free electron-induced enhancement η_{drude} , which was calculated by modifying Eq. (4) for different tensile strains ζ . (b) Core electron-induced enhancement η_{core} , where $\eta_{core} = \eta - \eta_{drude}$.

therefore the overall effect of strain and electron density reduction is positive. We note that these results are similar to those previously found for strain effects on the localized surface plasmon resonance wavelength for gold nanospheres, in which under symmetric stretching, the reduction in core electron density blue shifted the plasmon resonance wavelength, while a red shift was predicted due to a decrease in the free electron density.²¹

An alternative explanation for the strain-induced SPP propagation enhancement in gold can be obtained by considering both the effects of intrinsic absorption, as well as the oscillation strength of SPPs. Specifically, the decrease of the free electron density induced by stretching the gold nanowire leads to relatively weaker collective oscillations of the free electrons, and as a result, the SPP excitation strength under visible light is weaker than would be for unstrained nanowires. From this point of view, we expect a reduced SPP propagation length due to a decrease in the free electron density. On the other hand, the interband transition losses in the visible spectrum around 500 nm (Ref. 36) are relatively large for gold, particularly as compared to silver. The energy band formed by the core electrons, which is accounted for in the core dielectric term, is minimally altered by the tensile strain. Therefore, the reduced core electron density implies that fewer electrons jump from the d -band to the sp -band, resulting in the occurrence of fewer interband transitions, which greatly lowers the absorption of the gold nanowires. The overall effect is, as previously discussed, an improvement in the efficiency for SPP propagation for wavelengths around 540 nm.

We close by noting that it is well-known that silver is an optically superior metal to gold at optical frequencies due to having lower interband transition losses. Because our proposed elastic strain engineering strategy succeeds by greatly reducing the interband losses in the core dielectric term, a significant enhancement for the SP propagation length due to strain is not expected for silver.

In conclusion, we have utilized an analytical waveguide model in conjunction with strain-induced variations in the core and free electron densities to demonstrate that substantial enhancements in the surface plasmon propagation lengths in gold nanowires at optical frequencies can be achieved through application of uniaxial mechanical strain. The substantial reduction in energy loss is found to be due to the reduction in core electron density, and results in a size-independent propagation length enhancement as a function of applied tensile strain. The present results provide a different avenue of exploration in order to achieve effective signal transfer at optical frequencies.

H.S.P. and X.B. both gratefully acknowledge NSF Grant No. CMMI-1036460 in support of this research. Both authors also acknowledge Professor Jen Dionne to bringing this topic to our attention. X.B. also thanks Dr. Stephen K. Gray for helpful discussions on the numerical solutions of the analytical waveguide model.

- ¹S. Maier, *Plasmonics: Fundamentals and Applications* (Springer, 2007).
- ²J. Weeber, Y. Lacroute, and A. Dereux, *Phys. Rev. B* **68**, 115401 (2003).
- ³L. Novotny and B. Hecht, *Principles of Nano-Optics* (Cambridge University Press, 2006).
- ⁴D. Gramotnev and S. Bozhevolnyi, *Nature Photon.* **4**, 83 (2010).
- ⁵S. Bozhevolnyi, *Plasmonics and Metamaterials* (Optical Society of America, 2008).
- ⁶W. L. Barnes, A. Dereux, and T. W. Ebbeson, *Nature* **424**, 824 (2003).
- ⁷S. Bozhevolnyi, V. Volkov, E. Devaux, J. Laluet, and T. Ebbesen, *Nature* **440**, 508 (2006).

- ⁸A. Boltasseva, T. Nikolajsen, K. Leosson, K. Kjaer, M. Larsen, and S. Bozhevolnyi, *J. Lightwave Technol.* **23**, 413 (2005).
- ⁹R. Oulton, V. Sorger, D. Genov, D. Pile, and X. Zhang, *Nature Photon.* **2**, 496 (2008).
- ¹⁰L. Liu, Z. Han, and S. He, *Opt. Express* **13**, 6645 (2005).
- ¹¹T. Nikolajsen, K. Leosson, and S. Bozhevolnyi, *Appl. Phys. Lett.* **85**, 5833 (2004).
- ¹²K. Tanaka and M. Tanaka, *Appl. Phys. Lett.* **82**, 1158 (2003).
- ¹³K. Leosson, T. Nikolajsen, A. Boltasseva, and S. Bozhevolnyi, *Opt. Express* **14**, 314 (2006).
- ¹⁴C. Zou, F. Sun, Y. Xiao, C. Dong, X. Chen, J. Cui, Q. Gong, Z. Han, and G. Guo, *Appl. Phys. Lett.* **97**, 183102 (2010).
- ¹⁵A. Manjavacas and F. Garcia de Abajo, *Nano Lett.* **9**, 1285 (2009).
- ¹⁶S. Maier, P. Kik, and H. Atwater, *Appl. Phys. Lett.* **81**, 1714 (2002).
- ¹⁷J. Khurgin and G. Sun, *Appl. Phys. Lett.* **96**, 181102 (2010).
- ¹⁸D. Solis, Jr., W. Chang, B. Khanal, K. Bao, P. Nordlander, E. Zubarev, and S. Link, *Nano Lett.* **10**, 3482 (2010).
- ¹⁹B. Wild, L. Cao, Y. Sun, B. Khanal, E. Zubarev, S. Gray, N. Scherer, and M. Pelton, *ACS Nano* **6**, 472 (2012).
- ²⁰C. F. Bohren and D. R. Huffman, *Absorption and Scattering of Light by Small Particles* (Wiley-Interscience, 1983).
- ²¹X. Qian and H. S. Park, *J. Mech. Phys. Solids* **58**, 330 (2010).
- ²²X. Qian and H. S. Park, *Nanotechnology* **21**, 365704 (2010).
- ²³H. S. Park and X. Qian, *J. Phys. Chem. C* **114**, 8741 (2010).
- ²⁴K. Sturm, E. Zaremba, and K. Nuroh, *Phys. Rev. B* **42**, 6973 (1990).
- ²⁵J. Lerme, M. Pellarin, E. Cottancin, M. Gaudry, M. Broyer, N. D. Fatti, F. Vallee, and C. Voisin, *Eur. Phys. J. D* **17**, 213 (2001).
- ²⁶W. Cai, H. Hofmeister, and M. Dubiel, *Eur. Phys. J. D* **13**, 245 (2001).
- ²⁷P. B. Johnson and R. W. Christy, *Phys. Rev. B* **6**, 4370 (1972).
- ²⁸E. A. Coronado and G. C. Schatz, *J. Chem. Phys.* **119**, 3926 (2003).
- ²⁹Y. Yue, P. Liu, Z. Zhang, X. Han, and E. Ma, *Nano Lett.* **11**, 3151 (2011).
- ³⁰J.-H. Seo, Y. Yoo, N.-Y. Park, S.-W. Yoon, H. Lee, S. Han, S.-W. Lee, T.-Y. Seong, S.-C. Lee, K.-B. Lee *et al.*, *Nano Lett.* **11**, 3499 (2011).
- ³¹G. Richter, K. Hillerich, D. S. Gianola, R. Monig, O. Kraft, and C. A. Volkert, *Nano Lett.* **9**, 3048 (2009).
- ³²A. M. Leach, M. McDowell, and K. Gall, *Adv. Funct. Mater.* **17**, 43 (2007).
- ³³H. S. Park and J. A. Zimmerman, *Phys. Rev. B* **72**, 054106 (2005).
- ³⁴H. S. Park, K. Gall, and J. A. Zimmerman, *J. Mech. Phys. Solids* **54**, 1862 (2006).
- ³⁵C. Pfeiffer, E. Economou, and K. Ngai, *Phys. Rev. B* **10**, 3038 (1974).
- ³⁶P. West, S. Ishii, G. Naik, N. Emani, V. Shalaev, and A. Boltasseva, *Laser Photonics Rev.* **4**, 795 (2010).